Electrochemical engineering of anodic oxygen evolution in molten oxides

Antoine Allanore [i,1]
[i] Department of Materials Science & Engineering
Massachusetts Institute of Technology,
77 Massachusetts Avenue, #13-5066, Cambridge, MA, 02139
allanore@mit.edu,
Phone: +1 617 452 2758

Keywords: molten oxide electrolysis, oxide melts, metal extraction, oxygen evolution, electrochemical engineering

Abstract

Molten oxide electrolysis (MOE) is a metal extraction process that exhibits an exceptionally high productivity in comparison with other electrowinning techniques. Furthermore, MOE has the ability to generate oxygen as an environmentally benign byproduct, which is a key asset to improve metal extraction sustainability. From an electrochemical engineering standpoint, the high concentration of metal cations dissolved in the electrolyte justifies cathode current densities above 10 000 $A.m^{-2}$. At the anode, the available data suggest a mechanism of oxidation of the free oxide anions which concentration in oxide melts is reported to be limited. In this context, the application of available mass-transfer correlations for the anodic oxygen evolution suggests a key role of convection induced by gas bubbles evolution.

[1] ISE member

Table of Content

1. Introduction

Society environmental awareness, in particular the issue of greenhouse gases emissions, is a strong incitation for the extractive metallurgy sector to reconsider its core processes. Metals and mining industries were indeed among the largest industrial GHG emitters in 2010 in the USA [1]. In this context, electrolytic techniques have been put forward for example by the steel industry as a mean to take benefit of future 'decarbonated' electricity. Among innovative electrochemical processes, molten oxide electrolysis (MOE) is the only concept that enables the direct reduction of oxide feedstock to liquid metal, a key asset for high-throughput metal production. The concept relies on the ability of a mixture of molten oxides - hereafter designated as melts or electrolyte - to dissolve significant amount of the oxide feedstock of interest and operate at a temperature higher than the targeted metal melting point. This technique has been investigated for the production of ferromanganese [2] or titanium [3]. One of the recent development of MOE is for iron, which has been produced in the liquid phase [4] along with oxygen gas [5] at current densities higher than 10 000 $A.m^{-2}$ in laboratory-scale cells. Such exceptional current densities are key to lower the footprint of the foreseen industrial scale process, but also raise interesting questions from an electrochemical engineering standpoint.

The net reactions on the cathode (1) and the anode (2) provide a macroscopic description of MOE where M is the targeted metal:

$$M^{n+} + ne^{-} \rightarrow M(l) \quad (1)$$

$$nO^{2-} \rightarrow \frac{n}{2}O_2(g) + 2ne^- \quad (2)$$

The concentration of metal cations feedstock (M^{n+}) in the electrolyte is high (C_{bulk}~ 3 000 mol.m^{-3}, see [4]) though the corresponding oxide represent typically less than 10% of the total oxide content. The order of magnitude of metal cation diffusivity is similar to the one observed in aqueous solutions, for example D_{Fe}^{2+}~10^{-9} m^2.s^{-1} in melts at 1600°C [6]. The specific value depends on the melt composition and the metal cation valence, but available data suggest that such order of magnitude is of relevance for most cations and melts investigated so far. Assuming a Nernst model of the cathode interface (Nernst layer thickness of δ=5.10^{-5} m), it is possible to estimate the limiting cathode current density for reaction (1) via:

$$j_{\lim} = nF\frac{D}{\delta}C_{bulk} \quad (3)$$

In the foreseen conditions the limiting cathode current density is predicted to excess 10 000 A.m^{-2}, in agreement with previous experimental reports [4].

The anodic oxygen evolution reaction (2) requires more careful examination. First, the chemistry of oxygen in molten oxides is unclear and compelling arguments are lacking to establish the exact nature of the reactant. Second, the generation of oxygen gas on the anode is expected to influence the mass transfer conditions and is a topic of interest to a broad community.

In the following, it is proposed to discuss the electrochemical engineering aspect of the oxygen evolution reaction in the molten oxide supporting electrolytes in absence of the metal oxide feedstock. This approach is adopted in order to simplify the electrochemistry of the system, in which the simultaneous presence of several metal

cations (eg. Fe^{3+} and Fe^{2+}) can lead to complications, for example the potential existence of electronic conductivity [7]. The first part provides a review of the physical chemical properties of the candidate electrolyte in the temperature range of iron production by MOE. An overview of oxygen chemistry in oxide melts is also presented. The second part is dedicated to a summary of the literature on oxygen evolution in oxide melts. The last part is a discussion of the possible transfer phenomena that can arise when generating oxygen in such electrolytes, and their influence on the corresponding limiting current density.

2. Properties of molten oxides supporting electrolyte

The design of an electrolyte for MOE is an important task to optimize the energetic efficiency of the electrolysis as well as the stability of the refractory or the anode materials [5]. The supporting electrolyte components are oxides, encompassing: silica (SiO_2), alumina (Al_2O_3), magnesia (MgO) and calcia (CaO). In the recent developments, the concentration of magnesia is fixed at around 10wt%, so that a ternary diagram is suitable to represent some of the candidate electrolyte compositions (Figure 1, computed using the software FactSage™ [8]). Four liquidus projections have been plotted to illustrate the broad range of possible compositions and melting points. As a rule inherited from industrial operation with melts, a reasonable amount of superheat is needed to allow satisfactory transport properties during the reduction and the metal tapping step. In the example of MOE for steelmaking, most of the targeted

electrolyte compositions have a melting point lower than 1450°C for a process that operates at 1600°C.

The electrolyte cations do not have the same electronegativity and polarizability and can be classified as acidic or basic following the definition proposed by Lewis: the propensity of donating electrons. Basic metal cations act as network modifiers i.e. have the ability to partially decompose the network formed by a covalent compound, e.g. silica (silicon being a network former, see Figure 2a). An ionic melt is obtained by the addition of a basic oxide (e.g. calcia) to a network former as illustrated in Figure 2b. The covalent or ionic nature of a melt therefore depends on the relative concentration of each oxide and their respective basicity. The concept of melt basicity has been defined and detailed elsewhere [9], and in this work the optical basicity will be used [10] as a relative quantification of the melt basicity. It allows to identify a melt composition with a single number, in a manner analogous to pH in aqueous solutions [11].

The densities and viscosities of some electrolyte candidates have been measured and are available in a reference compilation [12]. The values at 1600°C are presented in Figure 4 as a function of the melts optical basicity which compositions are available in Table 1.

In comparison to typical electrolytes for electrowinning, the melts exhibit a high density above 2500 $kg.m^{-3}$, in contrast with cryolite-based electrolyte for aluminium at 960°C at around 2090 $kg.m^{-3}$ [13], or aqueous electrowinning in the order of 1000 $kg.m^{-3}$. Oxide electrolytes have a viscosity above 0.2 Pa.s in striking contrast with the aluminium electrowinning electrolyte ($2.5x10^{-3}$ Pa.s at 960°C). It is noticeable that

the kinematic viscosity of the oxide melts varies significantly with the concentration in each oxide. This feature is an asset to design an electrolyte with optimized transport properties.

3. Oxygen chemistry in molten oxides

Before discussing the chemistry of the reactant in reaction (2), it is proposed to summarize the knowledge on the product, oxygen gas, in oxide melts.

3.1 Molecular oxygen in oxide melts

As observed in aqueous solutions, oxygen gas can dissolve in molten oxides in the form of a diatomic molecule [14]. The concentration of molecular oxygen that can be achieved is called the 'physical solubility' and is governed by the partial pressure in the gas atmosphere in equilibrium with the melt, presumably following Henry's law at low concentration [15]. In absence of multivalent ions, the melt structure determines the solubility of oxygen, but its diffusion mechanism remains unclear. The molecular oxygen solubility has rarely been measured in silica-free melts in the range of temperature foreseen for MOE, and the value reported [16] for PbO-SiO_2 melts at 1250°C is below 100 $mol.m^{-3}$. The order of magnitude of the molecular oxygen diffusivity in CaO-SiO_2-Al_2O_3 at 1450°C has been measured at 10^{-9} $m^2.s^{-1}$ [17]. Both molecular oxygen concentration and diffusivity are predicted to increase as the optical basicity (i.e. the concentration of network modifiers) increases.

3.2 Oxide ions in oxide melts

The description of oxide melt structures is available elsewhere [9,17,18,19]. Oxide ions in molten oxides are the product of the reaction between network modifiers and formers as illustrated in Figure 2b. An increasing concentration of network modifiers (electropositive cations) added to a network former like silica lead to de-polymerization into smaller anionic species. At a critical concentration of network modifiers, free oxide ions can be formed. As illustrated in Figure 3, a multicomponent oxide melt is therefore expected to contain oxygen atoms in various configurations, ranging from polyatomic anionic species to free oxide ions. Three types of oxygen are distinguished 'bridging oxygen' (BO), 'non-bridging oxygen' (NBO) and 'free oxygen' ions. Numerous theoretical models have been proposed to predict quantitatively the concentration of each oxygen species in binary silicate melts [e.g. 20], though there is no comprehensive and universally accepted theory applicable to the whole range of composition presented in Figure 1. Experimental measurements are also scarce because of the corresponding technical challenge. Park and Rhee [21] used X-ray photoelectron spectroscopy of O_{1s} on $CaO\text{-}SiO_2$ and $CaO\text{-}Al_2O_3$ binaries quenched from 1600°C to evaluate the distribution of the oxide ions among the possible configurations. One conclusion that can be drawn from their investigation is that the concentration of free oxide ions in calcia-silica binary systems is low, reaching a maximum value for the most basic compositions (57% CaO - 43% SiO_2, optical basicity of 0.69) at around 320 $mol.m^{-3}$ [22]. In the remaining of the present document, and as a limiting case study, the concentration of free oxide ions in the melts will be assumed to be independent of the

composition and at an asymptotic value of 500 mol.m^{-3}. The diffusivity of oxygen as an oxide ion in calcia-silica-alumina melts has frequently been measured by permeation or radioactive tracer techniques [23], and the corresponding value extrapolated from 1450°C to 1600°C is around 10^{-9} m^2.s^{-1}.

A common feature of oxide melts is the inverse proportionality between the viscosity and the diffusivity of the constitutive ions, a Stokes-Einstein type of relation referred to as Eyring's relation in such medium. The oxide ion diffusivity can be evaluated assuming the effective diameter (λ) of the diffusing species is twice the one of O^{2-} (λ=2 × 2.8.10^{-10} m) [24]:

$$D = \left(\frac{kT}{\lambda} \right) \frac{\mathrm{I}}{\mu} \tag{4}$$

It has to be emphasized that relation (4) underestimates by a factor 10 the experimental data reported in [22]. For the rest of the study, such correction will be applied to relation (4), leading to the estimated diffusivity values presented in Table 1. Relation (4) is useful from an electrochemical engineering standpoint as it allows the estimation of the Schmidt number (Sc):

$$Sc = \frac{\upsilon}{D} = \frac{\mu}{\rho \cdot D} = \frac{\lambda}{kT} \frac{\mu^2}{\rho} \tag{5}$$

which at 1600°C and for any of the compositions of interest is higher than 5.10^5. This implies that molecular diffusion will limit the rate of oxygen ions transport: the diffuse layer thickness will always be much smaller than the hydrodynamic layer thickness.

4. Electrochemical generation of oxygen from molten oxides

It is beyond the scope of this paper to discuss the electrochemical methods that have been previously used to investigate oxygen generation from molten oxides, and only the main conclusions will be reported.

In order to investigate the role of melts physical chemical properties on metallurgical reaction kinetics, and in particular the possible involvement of electronic conductivity on phase boundary reactions, numerous electrochemical measurements of oxygen evolution have been reported [25][26], mostly in binary alkali-silicate mixture below 1400°C. With the exception of one reference [27], these pioneering reports obtained with 2 or 3 platinum wires electrodes and using chronoamperometric methods all mention the possible role of a dimerization reaction. This reaction is foreseen as necessary to maintain a sufficient concentration of free oxide ions close to the anode:

$$2(SiO_4)^{4-} = (Si_2O_7)^{6-} + O^{2-} \quad (7)$$

It must be noted however that there is a lack of compelling experimental evidences to support this assumption. No inflection in the current/potential curves that could indicate a mass transfer limitation have been reported, and an intermediate step of dissolved/adsorbed oxygen production has frequently been suggested, via:

$$O^{2-} = O* + 2e^- \quad (8)$$

followed by a recombination of O* to form the gas molecule. The commonly cited rate-controlling step is the diffusion of the free oxide ion to the electrode, though most reports stress the possible role of the convection induced by the oxygen evolution.

Later studies have been conducted to provide a fundamental understanding of silicate melts chemistry for geology. One of the most cited work is dedicated to the CaO-MgO-xSiO_2 ($1.25<x<3$) system at 1450°C [28], and provides a complete analysis of the electrochemical measurements. In particular, an estimation of the free oxygen reactant concentration (50 $mol.m^{-3}$) and diffusivity (5.10^{-10} $m^2.s^{-1}$) is proposed, data that have frequently been quoted since then. This work did not fundamentally reconsider the reaction mechanism proposed previously.

Subsequent works have been dedicated to glass melts characterization [29][30] at temperature around 1000°C, and did not revise the fundamental mechanism for oxygen generation, focusing on the possible oxidation of the anode material [31]. Moreover, all authors concluded that the oxygen evolution reaction was limited by the transport of the free oxide ions at the electrode.

5. Mass transfer limitations

Literature data on oxygen evolution in molten oxide are scarce but consistent with the model of oxygen generation from free oxide following equation (2). The exact prediction of the physical chemical properties of the free oxide ion and its concentration are not available with high accuracy, but their order of magnitude shall be sufficient to provide a first estimate of the corresponding limiting current density. In the following, the limiting current density will be calculated at 1600°C for a fixed value of the free oxide concentration, independent of the melt optical basicity, at 500 $mol.m^{-3}$. The oxygen ion diffusivity is calculated using a modified Eyring's relation (relation (4) multiplied by 10), as summarized in Table 1 along with other data of relevance.

The experimental current densities for oxygen evolution in molten oxides have previously been measured using a vertical wire anode typically immersed by around 1 cm, in a molten oxide electrolyte placed in a vertical tube furnace configuration which provides an homogeneous and constant hot zone at the selected temperature. From an electrochemical engineering standpoint, there is therefore no forced convection to the anode and presumably no natural convection due to temperature gradient as well.

5.1 Nernst model

The Nernst model (relation 3) applied in introduction to the cathode reaction can be transposed to the anode reaction assuming the same boundary layer thickness on both electrodes (*50 µm*). The corresponding limiting current density is presented in Figure 5 for the melts of interests. The noticeable variations are inherited from the difference in viscosity of the various melts, with the highest value at 8000 $A.m^{-2}$ obtained

for the most basic melts with the lowest viscosity. This generic approach illustrates that the anode reaction in molten oxide electrolysis requires dedicated investigation in order to justify the high anodic current density previously reported. One of the uncertainties in this model relies on the determination of the thickness of the boundary layer, which is the matter of the more elaborated models presented in the next sections.

5.2 Free-convection model

Free-convection is a relevant transport phenomena in the past experiments dedicated to oxygen evolution in MOE. In the multicomponent molten oxides where free oxygen is a minor contributor to the electrical conductivity [9], free-convection can arise due to the gradient of density inherited from the chemical reactions happening at the electrode surface. This is analogous to the natural convection induced by temperature difference and Ibl [32] and Newman [33] propose to apply the similarity principle to the electrochemical case. If the Schmidt number is high, the Sherwood number (Sh) is evaluated via:

$$Sh = 0.67 \cdot (Sc \cdot Gr)^{1/4} \tag{9}$$

with

$$Sh = \frac{k_D \cdot L}{D} \tag{10}$$

and the Grashof number (Gr) defined as:

$$Gr = \frac{g \cdot \Delta\rho \cdot L^3}{\rho \cdot \upsilon^2} \tag{11}$$

Correlation (9) is valid for a product (Sc.Gr) between 10^4 and 10^{12}, what is the case for any of the melts of interest. The corresponding limiting current densities are presented

in Figure 5 (curve 'lbl'), calculated using L as the anode immersion depth (1cm) and a density gradient $\Delta\rho$ of 20%. The computed data vary with the melt viscosity and are around 65 % lower than the one estimated with the Nernst model. Such result suggests that free-convection alone is not sufficient to sustain the high current densities reported for oxygen evolution in MOE.

5.3 Other contributions to mass-transfer during oxygen evolution

As mentioned in the early reports on oxygen evolution in molten oxides [25], a convective mass transfer contribution due to the gas evolution is likely to occur at high current densities. It is beyond the scope of this paper to review the topic of hydrodynamics of electrochemically generated gases [34] but it is important to evaluate the magnitude of the mass-transfer enhancement achievable by gas generation at the anode. Most experimental data and available models obtained in aqueous electrolytes [35, 36, 37] suggest a potential ten-fold increase in the mass-transfer coefficient for gas generation at a current density higher than 1000 $A.m^{-2}$. All things being equal, such ten-fold enhancement of the free-convection case (equation 9) would justify the experimental current density reported for oxygen evolution in molten oxides. Such conclusion however requires further experimental validation.

Independently from these electrochemical approaches, the issue of mass transfer to oxygen bubble has been investigating by the glass industry in the context of gas removal from silicate melts. In this context the generation of dissolved oxygen into the melt is obtained by metal cation reduction (e.g. Fe^{3+}) in order to increase the diameter of the gaseous inclusions and increase their rate of removal by buoyancy. A recent

publication in this field [38] has investigated the mass-transfer coefficient to an oxygen bubble rising in an oxide melt and growing due to the oxygen generation obtained by trivalent iron ions reduction ('fining' effect):

$$2Fe^{3+} + O^{2-} \rightarrow 2Fe^{2+} + \frac{1}{2}O_2(g) \quad (11)$$

The mass transfer coefficient in absence of fining which is the situation that corresponds to an oxygen bubble touching an anode in MOE, has been evaluated using the boundary layer theory for the creeping flow of bubbles. A large Peclet number (Pe) is required to justify this assumption:

$$Pe = \frac{2 \cdot r^3 \cdot g \cdot (\rho_L - \rho_G)}{3 \cdot D \cdot \mu} \quad (12)$$

For 2 mm diameter oxygen bubbles and the diffusivity and viscosity values compiled in Table 1, the Pe number is greater than 10^3 for the selected melts. With this assumption, the mass transfer coefficient to the bubble (Sh_b) can been evaluated following Levich [39]:

$$Sh_b = 0.651\sqrt{Pe} \quad (13)$$

$$Sh_b = \frac{2 \cdot r \cdot k_D}{D} \quad (14)$$

The transposition of this phenomenon to the electrolysis case requires the assumption that the rising bubble along the vertical anode has the ability to bring fresh reactant (free-oxide) toward the bubble location, i.e. the anode surface. The corresponding limiting current densities with a bubbles radius (r) of 1 mm are presented in Figure 5 (curve 'Levich'). Differences in viscosities for each melts lead to the abrupt variations already noticed for the previous models. In this model however, the predicted limiting

current densities are of the correct order of magnitude with respect to the experimental reports for MOE. This may be interpreted as a confirmation of the possible enhancement of the mass transfer by an order of magnitude with respect to the free-convection case. These results illustrate the key importance of the gas-induced convection on the ability to produce oxygen in molten oxides at the foreseen current densities.

6. Conclusions

Experimental results in molten oxide electrolysis with current densities higher than 10 000 $A.m^{-2}$ are qualitatively justified by classical electrochemical engineering for the cathode reaction because of the high concentration of metal cation reactant. The diffusivity of this reactant compensates the relatively high viscosity of the supporting electrolyte, leading to high transport properties. For the anode reaction, an overview of the literature on oxygen chemistry and electrochemistry in melts shows that the exact nature and concentration of the oxide-containing reactant is not yet ascertained and that available data are scarce. The most probable source of oxide is free-oxygen which is presumably at a low concentration, implying that the oxygen evolution is likely to be controlled by the reactant transport. This is in striking difference with the aqueous electrolysis case, in which the concentration of hydroxide ions or water is always large enough to sustain high current densities. The application of existing electrochemical engineering models with available data suggests that mass-transfer enhancement due to bubble evolution will be critical to sustain the high current densities observed in MOE. Such conclusions call for a systematic experimental investigation of oxygen chemistry in

oxide melts. In parallel, there is a need to design electrochemical set-up with controlled flow conditions to investigate the electrochemical generation of oxygen in oxide melts.

composition in mol %								
CaO	**MgO**	**Al_2O_3**	**SiO_2**	**optical basicity**	**dynamic viscosity (mPa.s)**	**density ($kg.m^{-3}$)**	**kinematic viscosity ($m^2.s^{-1}$)**	**diffusivity (Modified Eyring) ($m^2.s^{-1}$)**
11.1	14.0	11.1	63.9	0.550	8870	2575	3.44E-03	5.2E-11
25.9	10.5	8.3	55.3	0.590	1902	2694	7.06E-04	2.4E-10
18.7	24.2	11.7	45.5	0.605	800	2585	3.09E-04	5.8E-10
23.2	18.7	9.4	48.6	0.610	937	2666	3.51E-04	4.9E-10
30.0	12.4	14.1	43.6	0.620	984	2720	3.62E-04	4.7E-10
33.5	12.0	10.1	44.4	0.630	744	2705	2.75E-04	6.2E-10
34.0	12.0	10.0	44.0	0.632	432	2743	1.57E-04	1.1E-09
39.7	14.9	11.2	34.1	0.660	406	2749	1.48E-04	1.1E-09
38.9	14.6	10.9	35.6	0.661	406	2749	1.48E-04	1.1E-09
50.0	6.0	0.0	44.0	0.680	210	2651	7.92E-05	2.2E-09
39.9	12.3	17.3	30.5	0.690	295	2576	1.15E-04	1.6E-09
43.7	17.2	11.8	27.3	0.693	300	2766	1.08E-04	1.5E-09

Table 1. *Compositions and physical-chemical properties of some candidate electrolytes for MOE. Data are from [12] and models available therein.*

Figures Captions

***Figure 1**. Liquidus projections from 1250 to 1600°C for the quaternary system calcia - silica - alumina - magnesia (10wt%). Dots represent some of the compositions of interest for MOE, the numbers indicate their corresponding optical basicity.*

***Figure 2.** Schematic structural difference between a pure silica melt (a) and a more basic, ionic melt obtained by addition of a network modifier like calcia (b).*

***Figure 3.** Possible configurations of the oxide ion in a partially ionic melt (NBO: non-bridging oxygen, BO: bridging oxygen). The large spheres represent the oxygen ion*

***Figure 4**. Density, dynamic (left axis) and kinematic viscosities (right axis) of selected electrolytes at 1600°C ranked by their optical basicity.*

***Figure 5.** Variation of the limiting current density in melts of increasing basicity for the Nernst, free-convection ('lbl') and boundary layer ('Levich') models (1600°C, $[O^{2-}] = 500$ mol.m^{-3}, Nernst boundary layer of 50 µm, anode immersion of 1cm, bubbles radius 1mm).*

References

[1] Greenhouse Gas (GHG) Inventory in the United States in 2010, US Environment Protection Agency, available at http://www.epa.gov/climatechange/ghgemissions/usinventoryreport.html, last visit October 2012
[2] R. Winand, A. Fontana, L. Segers, L. Hannaert, J. Lacave, Molten salt electrolysis in metal production, Int. Symp. (1977) 42-50
[3] D.R Sadoway, Electrochemical processing of refractory metals, Journal of Metals, 43 (1991) 15
[4] D. Wang, A.J. Gmitter, D.R. Sadoway, Production of oxygen gas and liquid metal by electrochemical decomposition of molten iron oxide, J. Electrochem. Soc. 158 (2011) 51
[5] H. Kim, J. Paramore, A. Allanore, D.R. Sadoway, Electrolysis of molten iron oxide with an iridium anode: the role of electrolyte basicity, J. Electrochem. Soc. 158 (2011) 101
[6] R.F. Johnston, R.A. Stark, J. Taylor, Diffusion in liquid slags, J. Ironmaking & Steelmaking 4 (1974) 220
[7] M. Barati, K.S. Coley, Electrical and electronic conductivity of CaO-SiO_2-FeOx slags at various oxygen potentials: Part II. Mechanism and a model of electronic conduction, Metallurgical and Materials Transactions B, 37 (2006) 51
[8] C. W. Bale, A. D. Pelton, FactSage 6.1 (2009)
[9] Y. Waseda, J. M. Toguri, The Structure and Properties of Oxide Melts : Application of Basic Science to Metallurgical Processing, World Scientific, Singapore, River Edge, NJ 1998
[10] J. A. Duffy, A review of optical basicity and its applications to oxidic systems, Geochim. Cosmochim. Acta 57 (1993) 3961
[11] C.A. Angell, Electron free energy levels in oxidic solutions: relating oxidation potentials in aqueous and non-aqueous systems, J. Solid State Electrochem., 13 (2009) 981
[12] SlagAtlas, V.D.Eisenhuttenleute, 2nd edition,VerlagStahleisen 1995.
[13] A. Solheim, Light Metals 2011 Edited by: Stephen J. Lindsay TMS (The Minerals, Metals & Materials Society) (2011) 381
[14] R.H. Doremus, Diffusion in glasses and melts, Journal of Non-Crystalline Solids, 25 (1977) 261
[15] H.D. Schreiber, S.J. Kozak, A.L. Fritchman, D.S. Goldman, H.A. Schaeffer, Redox kinetics and oxygen diffusion in a borosilicate melt, Physics and Chemistry of Glasses 27 (1986) 152
[16] K. Sasabe, S. Goto, Permeability, diffusivity, and solubility of oxygen gas in liquid slag, Metallurgical Transactions, 5 (1974) 2225
[17] F.D. Richardson, Physical chemistry of melts in metallurgy, Academic Press, London, New York 1974
[18] E.T. Turkdogan, Physicochemical properties of molten slags and glasses, Metals Society, London 1983
[19] B.O. Mysen, P. Richet, Silicate Glasses And Metals: Properties And Structure, Elsevier, Amsterdam, 2005
[20] G.W. Toop and C.S. Samis, Activities of ions in silicate melts,Transactions of the Metallurgical Society of AIME 224 (1961) 878
[21] J.H. Park, P.C.H. Rhee, Ionic properties of oxygen in slag, Journal of Non-Crystalline Solids 282 (2001) 7-14
[22] A. J. Gmitter, Master Thesis in Material Science and Engineering, MIT, Cambridge (2008)
[23] P.J. Koros, T.B. King, The self-diffusion of oxygen in a lime-silica-alumina slag, Transactions of the Metals Society AIME 224 (1962) 299
[24] T. Dunn, Oxygen chemical diffusion in three basaltic liquids at elevated temperatures and pressures, Geochimica et Cosmochimica Acta 46 (1982) 2293
[25] A. Ghosh, T.B. King, Kinetics of oxygen evolution at a platinum anode in lithium silicate melts, Transactions of the Metallurgical Society of AIME 245 (1969) 145
[26] H. Siuto, M. Ohtani, Galvanostatic polarization measurements on a solid platinum-alkali silicate melts, Transactions of the Iron and Steel Institute of Japan, 17 (1977) 37
[27] M. Kawakami, K.S. Goto, Potentiostatic polarization measurements on solid platinum - molten PbO-GeO_2, PbO-SiO_2, and Na_2O-SiO_2 interfaces, Metallurgical Transactions 4 (1973) 1097

[28] K. W. Semkow, L. A. Haskin, Concentrations and behavior of oxygen and oxide ion in melts of composition $CaO.MgO.xSiO_2$ Geochimica et Cosmochimica Acta 49 (1985) 1897
[29] M. Maric, M.P. Brungs, M. Skyllas-Kazacos, Anodic voltammetric behaviour of a platinum electrode in molten sodium disilicate glass containing Fe_2O_3, Journal of Non-Crystalline Solids 105 (1988) 7
[30] J.-Y. Tilquin, J. Glibert, P. Claes, Anodic polarization in molten silicates, Journal of Non-Crystalline Solids 188 (1995) 266
[31] J.K. Higgins, Studies of platinum and molybdenum electrodes in molten silicates, borates, and phosphates, Journal of the Electrochemical Society 140 (1993) 3436
[32] N. Ibl, The use of dimensionless groups in electrochemistry, Electrochimica Acta, 1 (1959) 117
[33] J. Newman, Engineering design of electrochemical systems, Ind. Eng. Chem., 60 (1968) 12
[34] H. Vogt, in Yeager E., Bockris J. O. M., Conway B. E., Comprehensive treatise of electrochemistry Vol. 6, Plenum Press, New York (1983)
[35] S. Shibata, Supersolubility of hydrogen in acidic solution in the vicinity of hydrogen-evolving pliitinum cathodes in different surface states, Denki Kagaku, 44 (1976) 709
[36] H. Vogt, Thermal effect on liquid-phase free convection at gas evolving electrodes, International Journal of Heat Mass Transfer 36 (1993) 4115
[37] V.G. Nefedov, Mass transfer to a gas-generating electrode, Russian Journal of Electrochemistry, 34 (1998) 16
[38] F. Pigeonneau, Mass transfer of a rising bubble in molten glass with instantaneous oxidation–reduction reaction, Chemical Engineering Science 64 (2009) 3120
[39] V. G. Levich, Physicochemical hydrodynamics, Prentice-Hall Englewood Cliffs, NJ (1962)

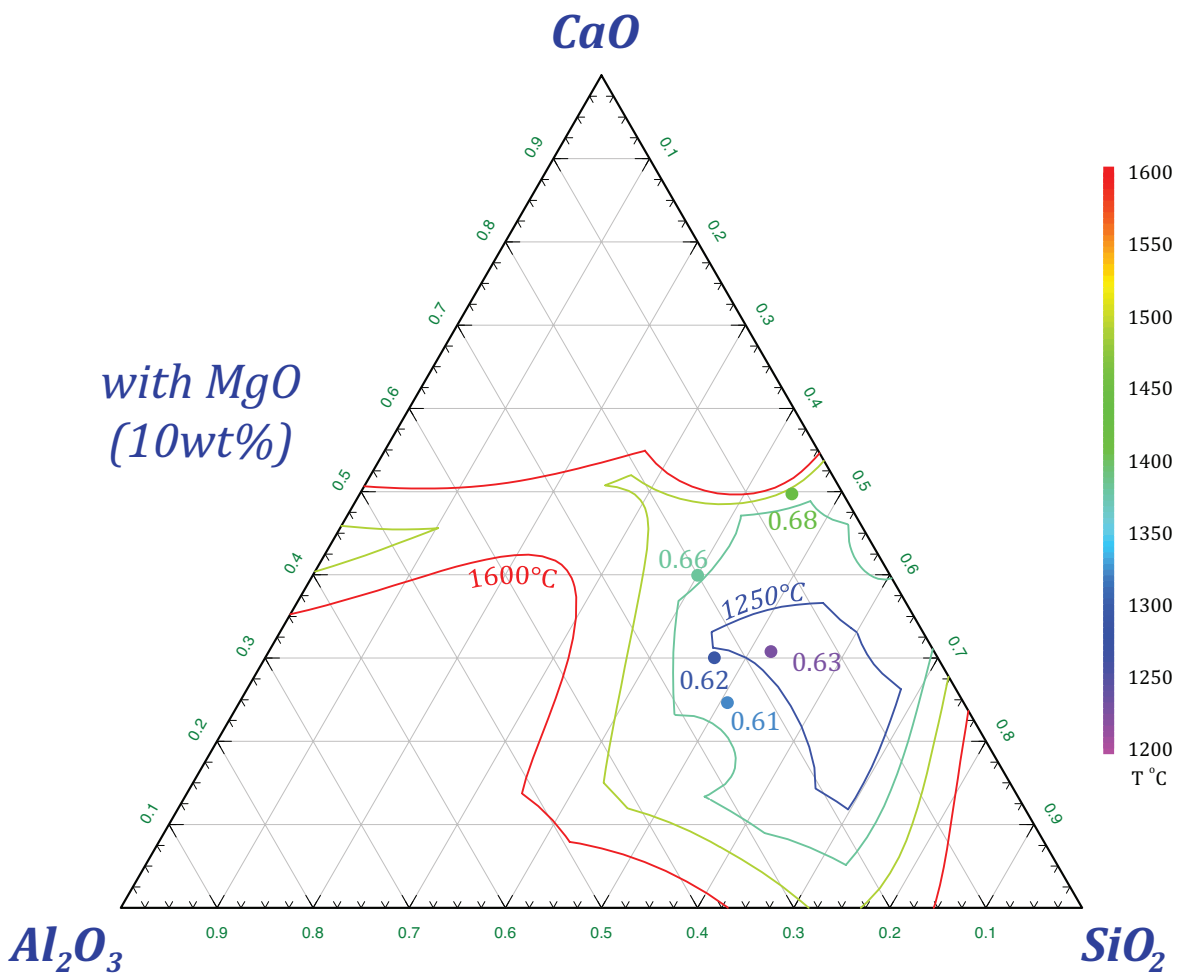

Figure 1. *Liquidus projections from 1250 to 1600°C for the quaternary system calcia - silica - alumina - magnesia (10wt%). Dots represent some of the compositions of interest for MOE, the numbers indicate their corresponding optical basicity*

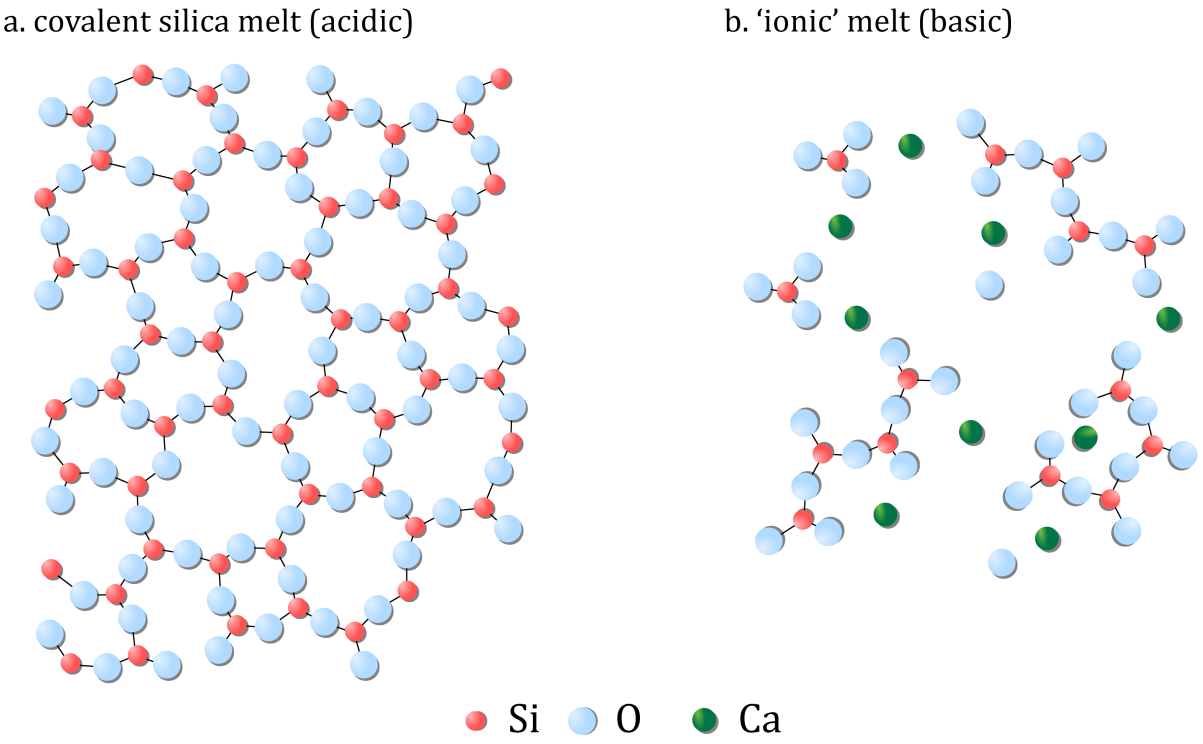

Figure 2. *Schematic structural difference between a pure silica melt (a) and a more basic, ionic melt obtained by addition of a network modifier like calcia (b)*

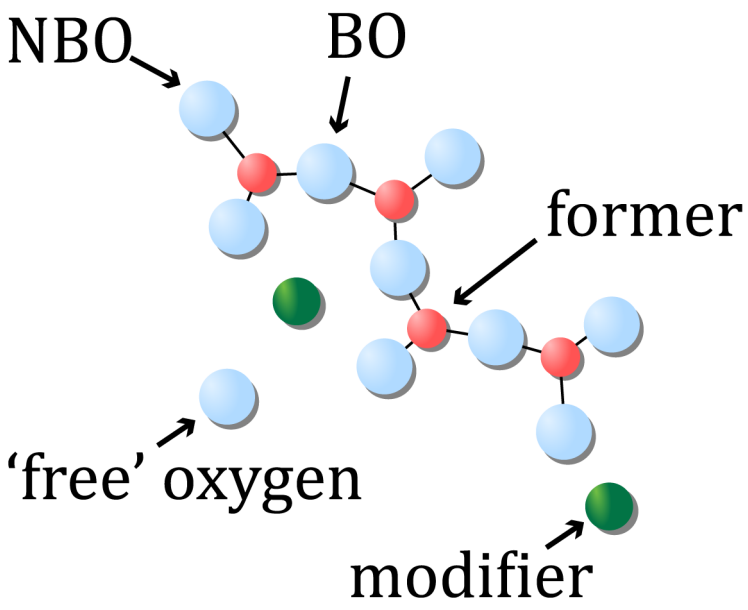

Figure 3. *Possible configurations of the oxide ion in a partially ionic melt (NBO: non-bridging oxygen, BO: bridging oxygen). The large spheres represent the oxygen ion.*

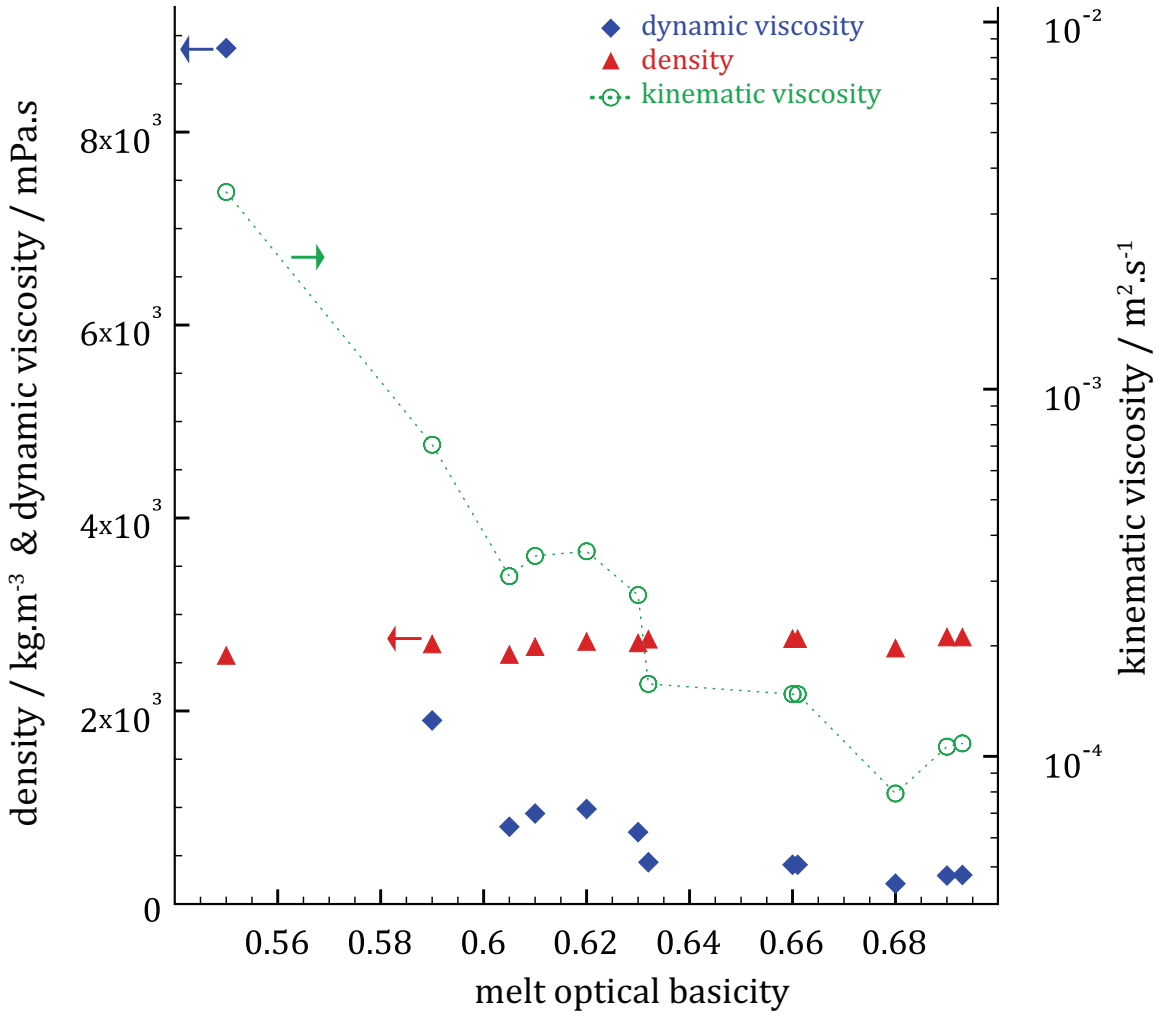

***Figure 4**. Density, dynamic (left axis) and kinematic viscosities (right axis) of selected electrolytes at 1600°C ranked by their optical basicity*

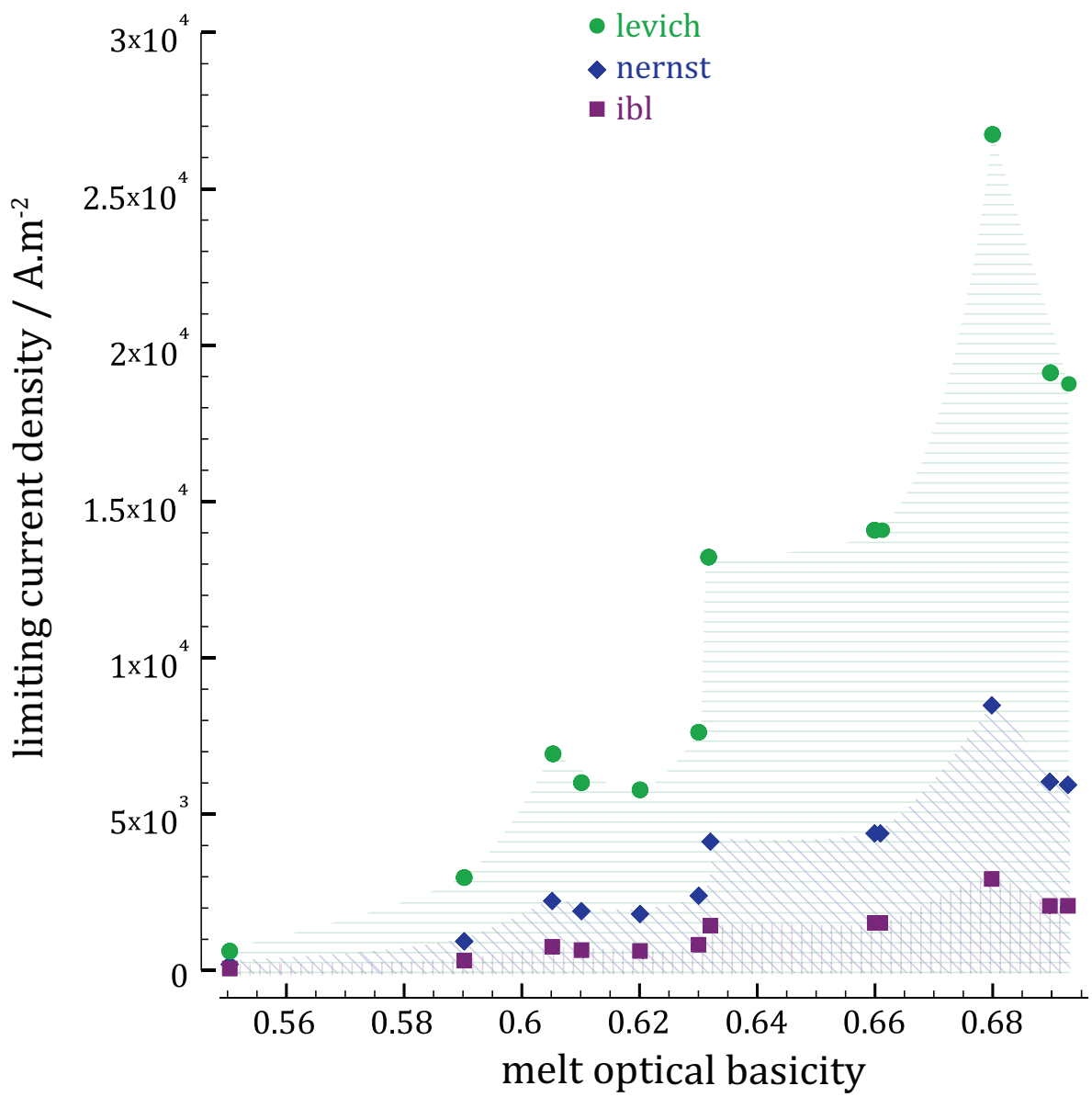

Figure 5. *Variation of the limiting current density in melts of increasing basicity for the Nernst, free-convection ('Ibl') and boundary layer ('Levich') models (1600°C, [O^{2-}] = 500 mol.m^{-3}, Nernst boundary layer of 50 µm, anode immersion of 1cm, bubbles radius 1mm)*